5 October 2001

ELSEVIER

Chemical Physics Letters 346 (2001) 274–282

CHEMICAL PHYSICS LETTERS

www.elsevier.com/locate/cplett

Simulation of quantum systems using path integrals in a generalized ensemble

Ioan Andricioaei [a,*,1], John E. Straub [b], Martin Karplus [a,c,*]

[a] *Department of Chemistry and Chemical Biology, Harvard University, 12 Oxford Street, Cambridge, MA 02138, USA*
[b] *Department of Chemistry, Boston University, Boston, MA 02215, USA*
[c] *Institut Le Bel, Université Louis Pasteur, Strasbourg, France*

Received 6 March 2001; in final form 20 June 2001

Abstract

The possibility of using path-integral simulations in a generalized ensemble based on the Tsallis statistics is explored. The primitive model algorithm with the Tsallis ensemble replacing the canonical ensemble converges to the quantum-mechanical result with a smaller number of beads in the isomorphic chain. Examples considered are the harmonic oscillator, two double-well systems and a double-well system immersed in an adiabatic solvent.

1. Introduction

There is considerable interest in the use of discretized path-integral simulations to calculate thermodynamical averages using quantum-statistical mechanics for many-body systems [1]. The theoretical basis of such methods is the Feynman path-integral representation [2] from which is derived the isomorphism between the equilibrium canonical ensemble of a quantum system and the canonical ensemble of a classical system of ring polymers of beads, or pseudo-particles. The classical system of ring polymers can be simulated with either Monte Carlo (MC) [3] or molecular dynamics [4] methods. Examples of the applications of such simulations are the studies of the quantum-mechanical contributions to the structure of water [5], the electron localization in water clusters [6], and the reaction rates for intramolecular proton transfer in acetylacetone [7].

For a system at temperature $T = 1/k_B\beta$ in the potential $V(x)$ and having the Hamiltonian operator $H \equiv K + V = -(\hbar^2/2m)\nabla^2 + V(x)$, the coordinate-representation elements, $\rho(x, x'; \beta) = \langle x|e^{-\beta H}|x'\rangle$, of the density matrix operator in the canonical ensemble are evolving in what is interpreted as an imaginary time β, according to the Bloch equation, $\partial\rho/\partial\beta = H\rho$, and satisfy

$$\int \rho(x_1, x_1; \beta)\,dx_1 = \int \dots \int \rho(x_1, x_2; \beta/P) \dots \rho(x_{P-1}, x_P; \beta/P) \times \rho(x_P, x_1; \beta/P)\,dx_1 \dots dx_P. \quad (1)$$

For large P, β/P is small and it is possible to find a good short-time approximation to ρ. This is usually done by employing the Trotter product

* Corresponding author. Fax: +1-617-496-3204.
E-mail addresses: andricio@tammy.harvard.edu (I. Andricioaei), marci@tammy.harvard.edu (M. Karplus).
[1] Fax: +1-617-496-4793.

0009-2614/01/$ - see front matter
PII: S0009-2614(01)00965-4

formula for the exponentials of the non-commuting operators K and V

$$e^{-\beta H} = \lim_{P\to\infty} \left(e^{-\beta K/P} e^{-\beta V/P}\right)^P. \tag{2}$$

In the so-called primitive representation of the discretized path-integral approach [2], the canonical partition function for finite P has the form

$$Q_P(\beta) \equiv \int \rho(x,x;\beta)\,dx = \left(\frac{mP}{2\pi\hbar^2\beta}\right)^{P/2} \times \int \cdots \int \exp\left\{-\beta\left(\left(\frac{mP}{2\hbar^2\beta^2}\right) \times \sum_{i=1}^{P} (x_i - x_{i+1})^2 + \frac{1}{P}\sum_{i=1}^{P} V(x_i)\right)\right\} dx_1 \ldots dx_P. \tag{3}$$

With neglect of the quantum effects that arise from the exchange of identical particles [8], Eq. (3) gives the exact quantum partition function for $P \to \infty$. For finite P, $Q_P(\beta)$ is the canonical partition function of a classical system composed of ring polymers. Each quantum particle corresponds to a ring polymer of P beads, in which neighboring beads are connected by harmonic springs with force constant $mP/2\hbar^2\beta^2$ and each bead is acted on by the interaction potential V/P. By simulating the classical system of ring polymers for a large enough value of P, meaningful convergence to the quantum-mechanical result can been achieved. Quantum thermodynamic averages can be calculated using appropriate estimators. For instance, the estimator $\mathscr{U}_P$ for the internal energy, $U = \langle \mathscr{U}_P \rangle$ (the average is over the canonical distribution), can be found using the thermodynamic relation, $U = -\partial \ln Q/\partial\beta$, by substituting $Q_P(\beta)$ for Q,

$$\mathscr{U}_P = \frac{P}{2\beta} - \frac{mP}{2\hbar^2\beta^2}\sum_{i=1}^{P}(x_i - x_{i+1})^2 + \frac{1}{P}\sum_{i=1}^{P} V(x_i). \tag{4}$$

For systems exhibiting sizeable quantum effects, a large value of P is needed. However, in addition to increasing the number of degrees of freedom for the polymer rings, this causes a slowing of the relaxation of the springs connecting the pseudo-particles [1]. Thus, methods to either reduce the number of beads or improve the sampling efficiency for a finite value of P are highly desirable. Several techniques have been devised for better convergence as a function of P. For systems with strongly repulsive interactions Barker [3] proposed and Pollock and Ceperley [9] implemented a short-time approximation scheme that replaces the potential V with a 'quantum' potential calculated by a numerical matrix multiplication; this scheme shows better convergence with increasing P for systems with hard-core repulsions. Reduction in the value of P that is required can also be achieved by renormalization techniques [10] or by choosing a higher-order short-time approximation [11]. Staging Monte Carlo (MC) [12], in which one grows the polymer ring in stages, is another useful technique for improved sampling. Normal mode decomposition has also been used for improving the sampling efficiency [13]. In addition, umbrella sampling techniques have been employed to reduce P [14]. All of these methods are within the framework of the standard primitive algorithm given in Eq. (3). We present here a method which generalizes the distribution of the classical ring polymers. On one hand, the method shows better convergence, and on the other hand it can be used as a framework for all the other schemes (normal modes, staging, etc.) that improve the standard primitive algorithm.

In previous work on enhanced configurational sampling, Straub and Andricioaei [15,16] have conjectured that a new method based on the Tsallis generalization of the canonical ensemble [17] would be expected to have faster convergence with P. In this Letter we outline the approach and demonstrate its performance for several model systems. Results of the implementation of the method for path-integral MC are presented, but corresponding generalizations of path-integral molecular dynamics algorithms and of centroid molecular dynamics methods [18] are straightforward. The latter is of particular interest as an approach to quantum dynamics.

2. Theory of the method

In the Tsallis generalization of the canonical ensemble [17], the probability density to be at position x is

$$p_q(x) \propto (1-(1-q)\beta V(x))^{1/1-q}, \tag{5}$$

which has the property that $\lim_{q\to 1}(1-(1-q)\beta V(x))^{1/1-q} = \exp(-\beta V(x))$; i.e., Boltzmann statistics is recovered in the limit of $q = 1$. For values of $q > 1$, the generalized probability distributions $p_q(x)$ are more delocalized [2] than the Boltzmann distribution at the same temperature (see Fig. 1). This feature has been used as the main ingredient for a set of successful methods to enhance the configurational sampling of classical systems suffering from broken ergodicity [23,24]. In what follows, we present the application of this approach to quantum systems simulated via the discretized path-integral representation.

If we put $P = 1/(q-1)$, the Tsallis probability density becomes

$$p_P(x) \propto \left(\frac{1}{1+\beta V(x)/P}\right)^P \tag{6}$$

and the sequence $P = 1, 2, 3, \ldots, \infty$ is equivalent to $q = 2, \frac{3}{2}, \frac{4}{3}, \ldots, 1$. Instead of a small imaginary time step for the standard density matrix operator, $e^{-\beta H/P} \simeq e^{-\beta K/P} e^{-\beta V/P}$, we write

$$e^{-\beta H/P} \simeq e^{-\beta K/P}\left(\frac{1}{1+\beta V(x)/P}\right) \tag{7}$$

which is exact up to order $(1/P)$ [16].

By defining

$$\bar{V} = \frac{P}{\beta}\ln\left(1+\frac{\beta}{P}V\right) \tag{8}$$

the generalized algorithm can be cast in a familiar form, in which the canonical partition function of the isomorphic classical system becomes

$$Q_P(\beta) \equiv \left(\frac{mP}{2\pi\hbar^2\beta}\right)^{P/2}\int\cdots\int e^{-\beta W_P}\,dx_1\ldots dx_P, \tag{9}$$

[2] Because of their power-law form (Lévy-like distributions [19] are obtained as stable distributions in the Tsallis formalism [20]), the generalized distributions appear naturally in systems with fractal properties of the relevant space and time [21]. Note that the structure of the chain of beads for highly quantum systems exhibits fractal scaling: the variance of a polymer chain of P beads equals P times the nearest-neighbor distance variance [22].

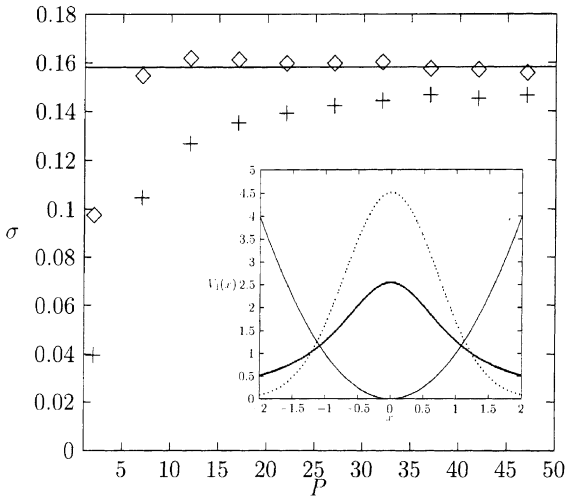

Fig. 1. The delocalization σ of the harmonic oscillator for various number of beads P, using the generalized (in diamonds) and the standard algorithm (in crosses). The continuous line is the exact quantum result for the standard deviation, calculated using Eq. (12). In the inset we show the probability density functions for a harmonic potential (drawn with a thin line) in the case of Boltzmann statistics, $q = 1$, (dotted line) and in the case of Tsallis statistics, $q = 2$ (thick line). The Tsallis statistics shows more delocalization than its regular counterpart.

where

$$W_P = \left(\frac{mP}{2\hbar^2\beta^2}\right)\sum_{i=1}^{P}(x_i - x_{i+1})^2 + \frac{1}{P}\sum_{i=1}^{P}\bar{V}(x_i). \tag{10}$$

As with the standard primitive path-integral algorithm, it is possible to use any MC and molecular dynamics method to calculate thermodynamical averages of quantum many-body systems by sampling the configuration space of the isomorphic classical ring polymers according to $\exp(-\beta W_P)$.

We note that the sequence limit $P \to \infty$ needed for convergence to quantum mechanics of the *standard* primitive algorithm (Eq. (3)) yields also the correct quantum mechanics for the *generalized* primitive algorithm which makes use of the propagator in Eq. (7). However, there exists a possible advantage in using the generalized kernel since it corresponds to a more delocalized distribution. In this regard, it is important to note that, for the case of a harmonic oscillator, the classical treatment in the standard primitive representation for

all finite P underestimates the delocalization of the particle [25]. Using the generalized algorithm, we show in applications to several model problems (see Sections 3 and 4) that faster convergence (with lower values of P) is obtained because of the fact that the p_q, for $q > 1$, are more delocalized functions than the Boltzmann distribution.

3. Harmonic oscillator in thermal equilibrium

To test the convergence properties of the generalized algorithm we consider a system of linear harmonic oscillators at temperature T. Each harmonic oscillator is a point particle of mass m moving in the potential $V_1(x) = m\omega^2 x^2/2$ with the classical frequency ω (see inset in Fig. 1). One can calculate the thermodynamic properties of this system from the exact quantum-mechanical partition function, $Q = (2\sinh(\beta\hbar\omega/2))^{-1}$. For the harmonic oscillator, the exact expression of the canonical partition function Q_P for finite P is also available [25], $Q_P = f^{P/2}/(f^P - 1)$, where $f = 1 + R^2/2 + \sqrt{4 + R^2}R/2$ and $R = \beta\hbar\omega/P$.

For all P the classical treatment underestimates the delocalization of the particle, as described by the second moment of the probability distribution. This is reflected in the lower value of the internal energy relative to the exact quantum result. The generalized method increases the delocalization and is expected, therefore, to result in faster convergence, as we show below. A good measure to quantify the delocalization of the quantum particle is the root mean square deviation of the beads from the center of mass x_{CM} of the polymer [4], calculated as

$$\sigma = \sqrt{\frac{1}{P}\sum_{i=1}^{P}(x_i - x_{\mathrm{CM}})^2}. \tag{11}$$

This delocalization, for different values of P, in the standard algorithm and the generalized Tsallis algorithm, is shown in Fig. 1, together with the quantum-mechanical result of the standard deviation of the average probability density [2],

$$\sigma_{\mathrm{qm}} = \sqrt{\frac{\hbar}{2m\omega\tanh(\beta\hbar\omega/2)}}. \tag{12}$$

In Fig. 2 we show the convergence of the harmonic oscillator internal energy to the exact quantum result, $(\hbar\omega/2)\coth(\beta\hbar\omega/2)$, in two cases:

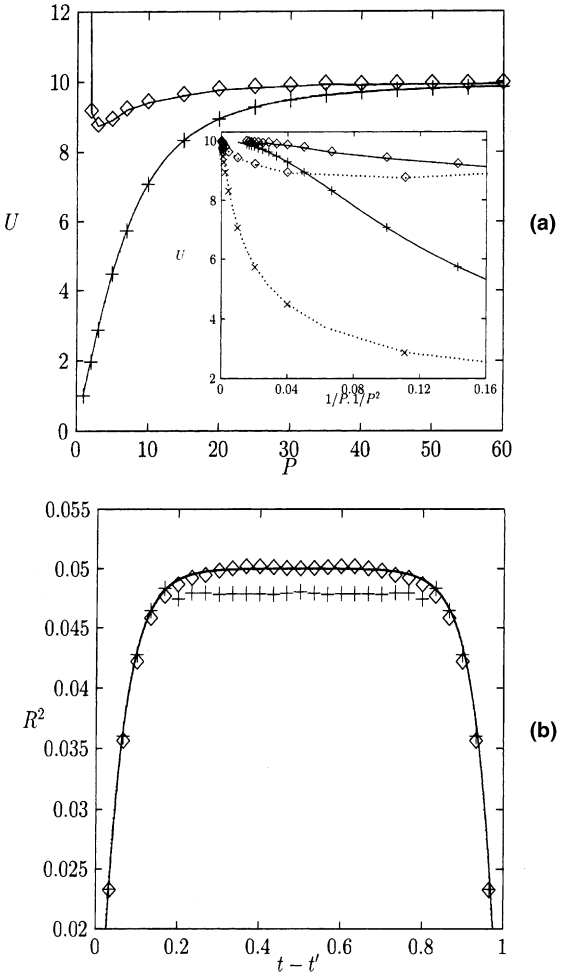

Fig. 2. (a) Internal energy per particle for the harmonic oscillator. The generalized method (in diamonds) converge faster to the exact quantum-mechanical result than does the standard one (in crosses). Parameters are $\omega = 20$, $T = 1$, $m = 1$. The inset compares the convergence of the internal energy for large P as a function of $1/P$ (continuous line) and $1/P^2$ (dotted line) (see text). (b) The displacement correlation function R^2 for the generalized algorithm (in diamonds) and for the primitive algorithm (in crosses), both with $P = 30$ beads, together with the exact result (continuous line). We used $\alpha = 5$ (see Eq. (13)) and we have ground state dominance with $\beta\hbar\omega = 20$. A value two times larger, $P = 60$, is required for the standard primitive algorithm to achieve the same convergence as the generalized method. Both algorithms ran for 20 000 MC cycles.

for a MC algorithm using the standard approach and for the generalized algorithm. Using the more delocalized Tsallis distributions, the internal energy is shown to be closer to the full quantum-mechanical result. The internal energy U was calculated as the average of the estimator in Eq. (4) over the distribution. With units such that $k_B = 1$ and $\hbar = 1$, for $T = 1$ and $\omega = 20$ the contribution of the first excited state is $\exp(-20)$ times that of the ground states; i.e., there is extreme dominance of the ground state. We performed 200 000 MC cycles which are enough for convergence for all the plotted values of P. One starts by constructing a string of P beads in one-dimension. They have a periodicity such that the string is closed, $x(P+1) = x(1)$. Each beads feels the harmonic potential V/P plus the spring potential from the two neighbors. Each bead is moved left or right, with the size of the move step randomly chosen from an interval $[-s_{\max}, s_{\max}]$, where $s_{\max}$ is varied every 100 steps such as to keep the acceptance of the moves to about 1/2. The inset of Fig. 2a shows the convergence of the internal energy as a function of $1/P$ and $1/P^2$. For both the generalized and the standard methods, the $1/P$ dependence is closer to a straight line on a larger interval of P values than the $1/P^2$ dependence, and reaches a plateau for large P. This is expected from the fact that both Eq. (7) and its standard counterpart are exact up to order $(1/P)$. Similar behavior is obtained for other convergence plots presented later in the Letter.

There exists the possibility that the delocalization resulting from the use of the Tsallis distribution overemphasizes the delocalization of the corresponding quantal system. This is the case when $P = 1$ for a harmonic oscillator, $V = x^2$. The Tsallis probability density is the Cauchy–Lorentz distribution, $1/(1+\beta x^2)$, whose second moment diverges. As a result the internal energy can be higher than the exact result. This can be seen in Fig. 2 and in the figures for the internal energy of the systems discussed in Sections 4.1 and 4.2. As P increases, there exists a critical value P_c with the property that the quantum delocalization is close to the one of the Boltzmann distribution for $P > P_c$ and overestimated relative to the Boltzmann distribution for $P < P_c$. One expects the Tsallis algorithm to be accurate for $P > P_c$ and most effective for a value of P near P_c, for which the number of beads is the smallest possible. Since the parameter controlling the delocalization is $q(P)$, one should choose the decay schedule of $q(P)$ optimally in practical applications. This is analogous to simulated annealing, where one chooses the optimum cooling schedule for the temperature decay. Here we introduce the 'cooling schedule' of q for the appropriate Tsallis distribution by using

$$q(P) = 1 + 1/\alpha P, \tag{13}$$

rather than $q(P) = 1 + 1/P$. We show an example of the effect of an optimal choice of the parameter α in Section 4.1.

In Fig. 2 we also plot the displacement correlation function,

$$R^2(t-t') = \langle |\mathbf{r}_i - \mathbf{r}_{i'}|^2 \rangle, \tag{14}$$

where $|i - i'| = (P/\beta\hbar)(t-t')$. $R^2(t-t')$, the mean-square distance between two beads of the chain separated by an Euclidean time increment $0 \leqslant t - t' \leqslant \beta\hbar$, is useful for the calculation of absorption spectra [26]. We compare the numerical MC results for the harmonic oscillator using the generalized and standard algorithm with the analytical formula for the harmonic oscillator [22]

$$R^2(t-t') = \hbar/(m\omega)\coth\left(\frac{\beta\hbar\omega}{2}\right) - \frac{\hbar/m\omega}{\sinh(\beta\hbar\omega/2)} \times \cosh\left(\frac{\beta\hbar\omega}{2} - \omega(t-t')\right). \tag{15}$$

The results demonstrate that an accurate correlation function can be obtained by the generalized algorithm with a significantly lower number of beads than in the standard algorithm.

4. Quantum systems in bistable potentials

4.1. Internal energy of a double oscillator system

A property that is of great interest in many reactions, particularly those involving proton transfer, is the contribution of tunneling. As a simple example we have considered a quantum particle in the one-dimensional double-well potential

$$V_2(x) = \frac{1}{2} m\omega^2 (|x| - a)^2, \tag{16}$$

shown in Fig. 3. It could model a diatomic molecule, (with positive and negative values of x corresponding to quantal barrier penetration of one particle through the other) or a symmetric hydrogen bond.

The isomorphic classical system was simulated with the MC algorithm to obtain U numerically, using the standard and the generalized algorithm. Initial positions of the particles in the polymer ring were randomly chosen in the interval $[-a, a]$. We ran 200 000 MC cycles and used an adaptative step size to keep the acceptance ratio around 1/2. Fig. 3 shows the internal energy U of the double oscillator in the potential $V_2(x)$ as a function of P. Together with the MC results, the quantum-mechanical internal energy result calculated by solving the corresponding Schroedinger equation is presented. We used as a basis set the first 15 harmonic oscillator eigenfunctions to construct the Hamiltonian matrix of the double-well system and diagonalized it to find its eigenvalues. To optimize the convergence, we have varied the parameter α in Eq. (13). A value of $\alpha = 0.6$ shows that a reduction by an order of magnitude in the number of beads is feasible with the generalized algorithm. For the case of the simulation whose results are shown in Fig. 3, the internal energy stays within 1% of the exact quantum result for $P > 70$ in the case of the standard MC scheme, while values of $P > 30$ are needed for the same accuracy when we use the generalized algorithm.

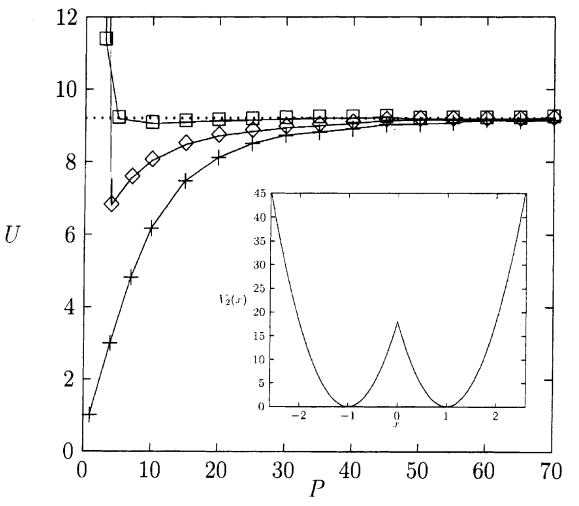

Fig. 3. Internal energy of the double oscillator, as a function of the number of beads, with $a = 0.4$, $kT = 1$, $\hbar\omega = 20$. The generalized algorithm results are shown in diamonds ($\alpha = 1$) and squares ($\alpha = 0.6$), the ones obtained using the standard primitive algorithm are in crosses. The inset shows the double oscillator potential $V_2(x)$ (Eq. (16)).

For a temperature $T = 1$ with $\beta\hbar\omega = 20$, only the lowest two eigenvalues contribute significantly (see above) and the partition function can be written:

$$Q = \exp\left(-\beta E^{(0)} - \frac{\Delta E}{2}\right) + \exp\left(-\beta E^{(0)} + \frac{\Delta E}{2}\right) \tag{17}$$

with $E^{(0)} = \hbar\omega/2$ and ΔE, the energy splitting of the ground state due to tunneling. The analytic expression for the internal energy ($U = -\partial \ln Q/\partial\beta$) is

$$U = E^{(0)} - \frac{\Delta E}{2} \tanh\left(\frac{\beta \Delta E}{2}\right). \tag{18}$$

We also plot, in Fig. 4, the results of the calculation of the tunnel splitting ΔE from Eq. (18) corresponding to the parameters in Fig. 3.

4.2. Internal energy of a quartic bistable system; coupling to an adiabatic solvent

To show that the fast convergence with P is not restricted to linear or piecewise-linear differential equations (see Figs. 1 and 3), we have performed simulations for the quartic bistable potential

$$V_3(x) = \frac{1}{8} \frac{m\omega^2}{a^2} (x - a)^2 (x + a)^2 \tag{19}$$

illustrated in Fig. 5. It is a widely used test system for approximate quantum calculations, although there is no exact analytic solution. We calculate the internal energy $U = -\partial \ln Q/\partial\beta$ of the quantum system using the standard primitive algorithm and the generalized one for different values of P by MC techniques. The result for U shown in Fig. 5a converges to the exact quantum-mechanical result, $U = 7.92$, obtained by solving numerically the

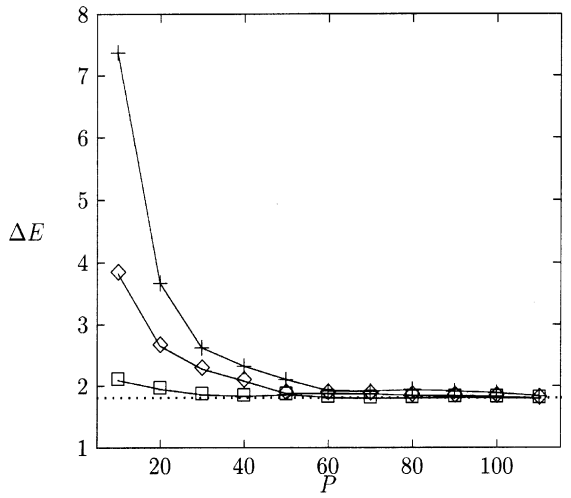

Fig. 4. Tunnel splitting for the standard algorithm (in crosses), and the generalized algorithm ($\alpha = 1$ in diamonds, and $\alpha = 0.6$ in squares), together with the exact splitting $\Delta E = 1.78$ (dotted line) calculated from the eigenvalues of the Schroedinger equation. Parameters are $a = 0.4$, $\omega = 20$.

corresponding Schroedinger equation. The parameters used were $\omega = 20$, $\beta = 1$, $a = 0.5$. As in the case of the double oscillator system, the convergence as a function of P is more rapid with the Tsallis ensemble than the standard primitive method.

The quartic potential $V_3(x)$ system was then coupled to a fluctuating adiabatic bath that represents the solvent, i.e., the time scale of the fluctuations of the bath is much longer than the relaxation time of the double-well system. This model, which has been used previously in path-integral calculations [10,25], has a coupling energy of the form $-\mu\mathscr{E}$, where $\mu = x/|x|$ is the dipole moment of the system and $\mathscr{E}$ is the electric field due to the bath. For each value of P, values of the random field $\mathscr{E}$ are taken from a Gaussian distribution, and the internal energy is averaged over the values of $\mathscr{E}$. The variance of the Gaussian distribution is chosen to be $2kT\sigma$, where σ is the solvation energy of the unit dipole. This spin-boson [22] system has non-trivial quantum properties, especially in the high tunnel-splitting regime, which are very difficult to simulate with the standard primitive scheme, in the sense that large values of P are needed.

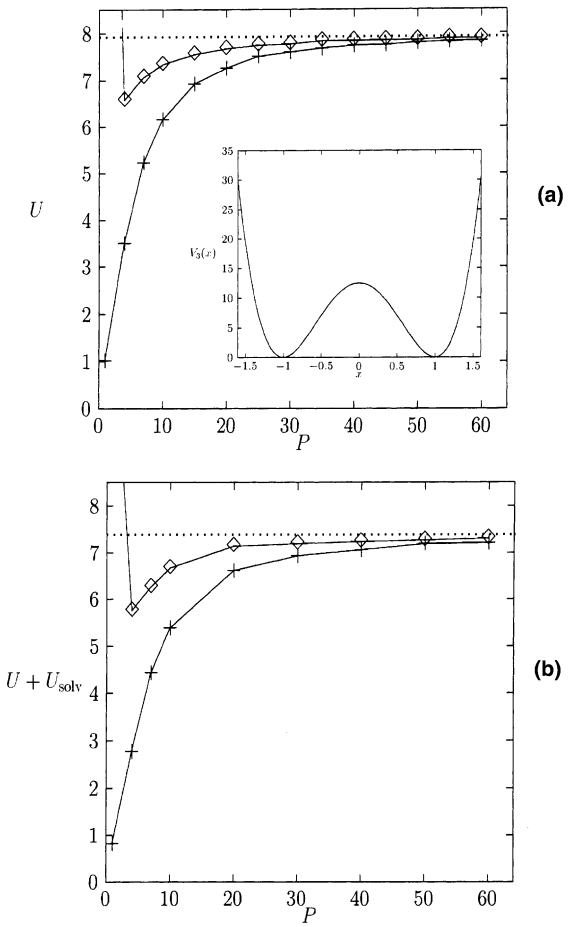

Fig. 5. Internal energy of isolated bistable system (a) and in fluctuating adiabatic solvent (b), for $\omega = 20$, $\sigma = 1$, $kT = 1$, $\alpha = 1$. The exact results are shown with dotted line. When the solvent was considered, we averaged over 500 Gaussian random values of $\mathscr{E}$ and ran for 200 000 MC sweeps at each value of $\mathscr{E}$. The inset shows the quartic bistable potential $V_3(x)$.

The quantum-mechanical partition function relative to the bath can be found analytically for the case of a two-level system (i.e., if $\hbar\omega \gg kT$) by mapping to an Ising model in a magnetic field [10,25] and has the expression

$$Z = \sqrt{1/\pi}\int_{-\infty}^{\infty} \mathrm{d}\Phi \mathrm{e}^{-\Phi^2} 2\cosh D, \tag{20}$$

where $D = \sqrt{(\beta\Delta E/2)^2 + 4\beta\sigma\Phi^2}$, and $\Phi = \sqrt{\beta/\sigma}\mathscr{E}/2$. The internal energy of solvation is thus

$$U_{\mathrm{solv}} = -\partial \ln Z/\partial\beta = \frac{\int_{-\infty}^{\infty} \mathrm{d}\Phi \mathrm{e}^{-\Phi^2} \sinh D(\beta(\Delta E/2)^2 + 2\sigma\Phi^2)/D}{\int_{-\infty}^{\infty} \mathrm{d}\Phi \mathrm{e}^{-\Phi^2} \cosh D}. \quad (21)$$

This result for U_{solv}, together with the solution of the Schroedinger equation for U are used to calculate a value of 7.386 for the internal energy of the system plus solvent. Convergence with the generalized Tsallis algorithm is much faster, as shown in Fig. 5b; i.e., convergence to within 1% of the quantum result is achieved by the algorithm at $P = 20$, while the standard algorithm requires values of $P > 50$ to achieve a similar degree of convergence. In the simulation, to keep the argument of the logarithm in Eq. (8) positive, a potential energy shift [24] was added to V and then removed at end of the simulation from the averaged result.

5. Discussion

By considering a number of quantum properties (delocalization, zero-point vibration, quantum thermodynamical averages, tunneling effects, quantum solvation) for several model systems, we have demonstrated that the generalized path-integral treatment based on using a Tsallis distribution with the primitive algorithm converges more rapidly as a function of the number of beads than the standard Boltzmann distribution. This is a consequence of the delocalization properties of the Tsallis probability density. We expect that the faster convergence properties of the generalized algorithm are conserved for more complex potentials so that the method has general applicability. Tests are now in progress for a parahydrogen solid, which displays many-body effects, as well as strong quantum behavior [27]. Although the Tsallis distribution is non-Boltzmann, we do not correct for this (i.e., we do not reweight the states such that averages of the Boltzmann distribution are calculated), in contrast to ordinary enhanced sampling algorithms based on non-Boltzmann distributions [28]. Instead, we use the Tsallis distributions as an approximation to the quantum-mechanical distribution, motivated by the fact that the Boltzmann distribution always underestimates the quantum-mechanical delocalization for the harmonic oscillator. This result is the principal motivation for the use of quantum effective potentials to enhance convergence in path-integral calculations. For instance, for systems with strong repulsions, the use of a quantum effective potential [3,9] is beneficial because it is a smoother version of the original 'bare' potential V. In other words, it is better if the potential term varies slowly (in space) relative to the kinetic term. The Tsallis effective potential $\bar{V}$ in Eq. (8), has this qualitative feature required, that is, it is a smoother version of V because of the logarithm which reduces high energy barriers.

For large systems we expect an additional benefit from the use of the generalized distribution. The centroids of the polymer rings move in these cases on a more rugged potential surface so that the sampling of the configurations should be enhanced in the generalized algorithm because of the smoother shape of the Tsallis effective potential; i.e., the corresponding classical distributions are more delocalized thus favoring faster escape from energy basins surrounded by large barriers [24]. This suggests that, in addition to a result closer to the quantum-mechanical case, the form of the propagator we have proposed should lead also to enhanced sampling of chain conformations relative to the standard primitive form. Moreover, for large P, the relaxation time of the polymer chain is large due to the stiffness of the bonds [1] (whose force constant increases with P), so that the generalized algorithm with lower P is expected to reduce this relaxation problem.

Since the computer time is approximately a linear function of P for distinguishable particles (and approximately quadratic for indistinguishable particles), an important speed-up in practical applications is expected because of the reduction in the number of beads.

Because the choice of the optimal 'cooling' schedule in Eq. (13) is crucial for practical applications, we now suggest a scaling formula for systems with n_{F} degrees of freedom. Following scaling arguments used for classical simulations with the Tsallis statistics [29], q should scale as

$1 + 1/n_F$. Consequently, we expect that α scales linearly with the number of degrees of freedom in multi-dimensional applications.

Acknowledgements

We are indebted to Professors David Coker and David Reichman, to Dr. Qiang Cui, and to Yisroel Brumer, Sara Bonella and Daniel Weinstock for valuable discussions and suggestions. The work was supported in part by a grant from the Department of Energy (MK) and the National Science Foundation CHE-9975494 (JES).

References

[1] B. Berne, D. Thirumalai, Ann. Rev. Phys. Chem. 37 (1986) 401.
[2] R. Feynman, A. Hibbs, Quantum Mechanics and Path Integrals, McGraw-Hill, New York, 1965.
[3] J. Barker, J. Chem. Phys. 70 (1979) 2914.
[4] M. Parrinello, A. Rahman, J. Chem. Phys. 80 (1980) 860.
[5] R. Kuharski, P. Rossky, Chem. Phys. Lett. 103 (1984) 357.
[6] D. Thirumalai, A. Wallqvist, B. Berne, J. Stat. Phys. 43 (1986) 973.
[7] K. Hinsen, B. Roux, J. Chem. Phys. 106 (1997) 3567.
[8] D. Ceperley, Rev. Mod. Phys. 67 (1995) 279.
[9] E. Pollock, D. Ceperley, Phys. Rev. B 30 (1984) 2555.
[10] D. Chandler, P. Wolynes, J. Chem. Phys. 74 (1981) 4078.
[11] H.D. Raedt, B.D. Raedt, Phys. Rev. A 28 (1983) 3575.
[12] M. Sprik, M. Klein, D. Chandler, Phys. Rev. B 31 (1985) 4234.
[13] M. Herman, E. Bruskin, B. Berne, J. Chem. Phys. 76 (1982) 5150.
[14] R. Friesner, R. Levy, J. Chem. Phys. 80 (1984) 4488.
[15] J.E. Straub, I. Andricioaei, Braz. J. Phys. 29 (1999) 179.
[16] I. Andricioaei, J.E. Straub, in: S. Abe, Y. Okamoto (Eds.), Nonextensive Statistical Mechanics and Its Application, Lecture Notes in Physics, Springer, Berlin, 2001, p. 195 (Chapter IV).
[17] C. Tsallis, J. Stat. Phys. 52 (1988) 479.
[18] J. Cao, G. Voth, J. Chem. Phys. 100 (1994) 5093.
[19] E. Montroll, M. Shlesinger, in: J. Lebowitz, E. Montroll (Eds.), Nonequilibrium phenomena II: From stochastics to hydrodynamics, North-Holland, Amsterdam, 1984, p. 1 (Chapter 1).
[20] C. Tsallis, S. Levy, A. Souza, R. Maynard, Phys. Rev. Lett. 75 (1995) 3589.
[21] M. Shlesinger, G. Zaslavsky, J. Klafter, Nature 363 (1993) 31.
[22] D. Chandler, in: D. Levesque, J. Hansen, J. Zinn-Justin (Eds.), Liquids, Freezing and Glass Transition, Elsevier, New York, 1990, p. 195.
[23] I. Andricioaei, J.E. Straub, Phys. Rev. E 53 (1996) R3055.
[24] I. Andricioaei, J.E. Straub, J. Chem. Phys. 107 (1997) 9117.
[25] K. Schweizer, R. Stratt, D. Chandler, P. Wolynes, J. Chem. Phys. 75 (1981) 1347.
[26] E. Gallicchio, B. Berne, J. Chem. Phys. 105 (1996) 7064.
[27] Y. Brumer, I. Andricioaei, D. Reichman, M. Karplus, to be published.
[28] G. Torrie, J. Valleau, Chem. Phys. Lett. 28 (1974) 578.
[29] U. Hansmann, Y. Okamoto, Braz. J. Phys. 29 (1999) 187.